Journal of Medicinal Chemistry

Article

pubs.acs.org/jmc

Discovery of Dihydrobenzoxazepinone (GS-6615) Late Sodium Current Inhibitor (Late I_{Na}i), a Phase II Agent with Demonstrated Preclinical Anti-Ischemic and Antiarrhythmic Properties

Jeff A. Zablocki,*[,†] Elfatih Elzein,[†] Xiaofen Li,[†] Dmitry O. Koltun,[†] Eric Q. Parkhill,[†] Tetsuya Kobayashi,[†] Ruben Martinez,[†] Britton Corkey,[†] Haibo Jiang,[†] Thao Perry,[†] Rao Kalla,[†] Gregory T. Notte,[†] Oliver Saunders,[†] Michael Graupe,[†] Yafan Lu,[†] Chandru Venkataramani,[†] Juan Guerrero,[†] Jason Perry,[⊥] Mark Osier,[§] Robert Strickley,[∥] Gongxin Liu,[#] Wei-Qun Wang,[#] Lufei Hu,[#] Xiao-Jun Li,[#] Nesrine El-Bizri,[#] Ryoko Hirakawa,[#] Kris Kahlig,[#] Cheng Xie,[#] Cindy Hong Li,[#] Arvinder K. Dhalla,[#] Sridharan Rajamani,[#] Nevena Mollova,[‡] Daniel Soohoo,[‡] Eve-Irene Lepist,[‡] Bernard Murray,[‡] Gerry Rhodes,[‡] Luiz Belardinelli,[#] and Manoj C. Desai[†]

[†]Medicinal Chemistry, [‡]Drug Metabolism, [§]Drug Safety Evaluation, [∥]Formulation and Process Development, and [⊥]Structural Chemistry, Gilead Sciences Inc., 333 Lakeside Drive, Foster City, California 94404, United States

[#]Biology, Gilead Sciences Inc., 7601 Dumbarton Circle, Fremont, California 94555, United States

Supporting Information

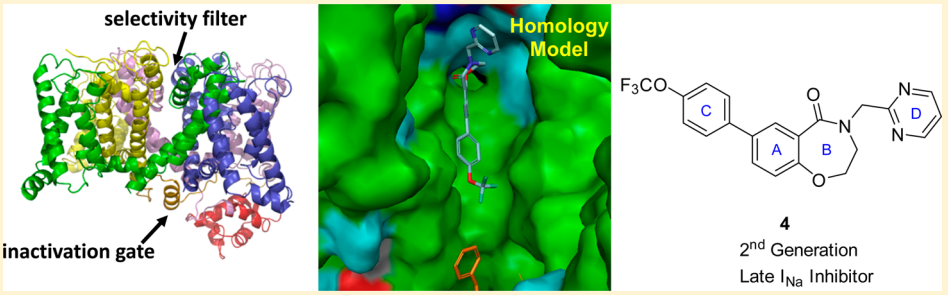

ABSTRACT: Late sodium current (late I_{Na}) is enhanced during ischemia by reactive oxygen species (ROS) modifying the Na_v 1.5 channel, resulting in incomplete inactivation. Compound **4** (GS-6615, eleclazine) a novel, potent, and selective inhibitor of late I_{Na}, is currently in clinical development for treatment of long QT-3 syndrome (LQT-3), hypertrophic cardiomyopathy (HCM), and ventricular tachycardia−ventricular fibrillation (VT−VF). We will describe structure−activity relationship (SAR) leading to the discovery of **4** that is vastly improved from the first generation late I_{Na} inhibitor **1** (ranolazine). Compound **4** was 42 times more potent than **1** in reducing ischemic burden in vivo (S−T segment elevation, 15 min left anteriorior descending, LAD, occlusion in rabbits) with EC_{50} values of 190 and 8000 nM, respectively. Compound **4** represents a new class of potent late I_{Na} inhibitors that will be useful in delineating the role of inhibitors of this current in the treatment of patients.

INTRODUCTION

The high prevalence (7%) of ischemic heart disease (IHD) in the United States (US) is a result of a western diet coupled with lack of exercise, resulting in atherosclerotic obstruction of coronary vessels.[1] Angina, a condition that afflicts nine million people in the US, is a symptomatic manifestation of IHD that causes chest pain.[2] Ranolazine **1** (Figure 1) was approved in the US in 2006 for the treatment of chronic angina.[3] Although the mechanism of **1**'s antianginal effect has not been determined, at therapeutic concentrations, **1** does inhibit cardiac late sodium current. Reactive oxygen species (ROS) generated during ischemia can modify the cardiac sodium channel resulting in incomplete inactivation of the channel allowing repetitive opening of the inactivation gate resulting in a persistent sodium current that occurs late in the action potential, thus termed late I_{Na} current (Figure 2).[4] Late I_{Na} current leads up to a 50% increase in cytoplasmic sodium that subsequently leads to Ca^{2+} overload through activity of the reverse mode Na−Ca^{2+} exchanger.[5] Compound **1** inhibits late I_{Na} current, thereby lowering the ischemic burden (calcium imbalance and sequelae).[5] At its therapeutic concentration (2−8 μM in plasma), **1** inhibits a number of cardiac ion currents (e.g., human *Ether-à-go-go*-related gene, hERG) and has β-blocker activity as well.[6] In preclinical models of ischemia, **1** has been shown to inhibit S−T segment elevation, a finding analogous to its ability to inhibit S−T segment changes in IHD patients with angina undergoing exercise treadmill testing (Monotherapy

Received: June 23, 2016

DOI: 10.1021/acs.jmedchem.6b00939
J. Med. Chem. XXXX, XXX, XXX−XXX

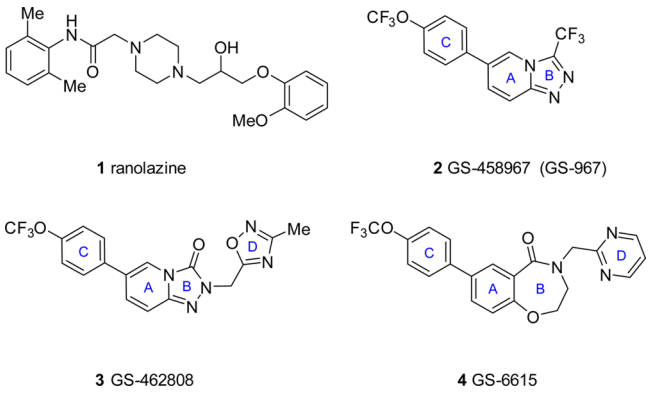

Figure 1. Gilead late sodium channel current (late I_{Na}) inhibitors progressed from **1** to a modified screening hit **2** with a narrow CNS margin, then to **3** with a wider CNS margin but a metabolic liability, followed by the development candidate **4** that meets all criteria.

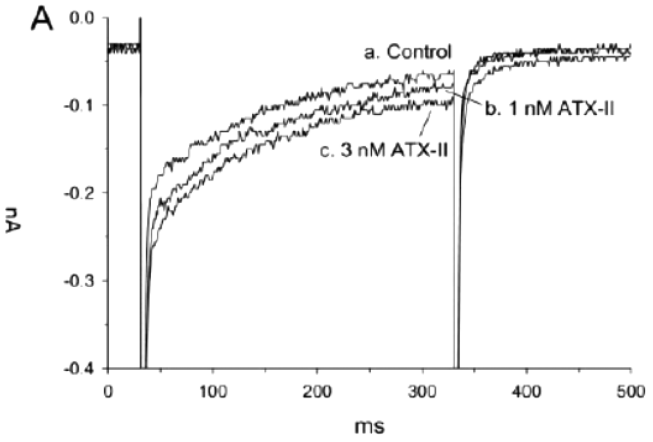

Figure 2. Late sodium current (Late I_{Na}) in a control experiment (a) or enhanced with aid of 1 nM (b) or 3 nM (c) ATX-II.

Assessment of Ranolazine In Stable Angina, MARISA Study).[7] We describe the discovery of a second-generation late I_{Na} inhibitor with improved properties relative to **1** with less hERG and β-blockade.

In site directed mutagenesis studies where the key phenylalanine or tyrosine of the lidocaine site have been independently mutated to alanine, **1** loses its inhibitory effect on late I_{Na} current, thus suggesting **1** binds at this site.[8] In vitro late I_{Na} current can be generated by the addition of toxins sea anemone toxin II (ATX-II) or tefluthrin that bind to an external binding site that does not overlap with the lidocaine binding site (Figure 2).[9] Compound **1** (Figure 1) has an IC_{50} of 6.9 μM for ATX-II induced late I_{Na} inhibition (single cell manual patch).[6] Peak I_{Na} current (peak cardiac sodium current) is responsible for the propagation of the action potential from cell to cell starting from the pacemaker sinoatrial (SA) node through the atria and ventricles. To avoid pro-arrhythmic effects, it is critical to have an adequate separation of late I_{Na} inhibition from peak I_{Na} current. Compound **1** has a separation of >50-fold for inhibition of late I_{Na} current relative to peak I_{Na} current, and it is important to maintain this separation.[6]

Herein, we describe our efforts to discover a potent late I_{Na} current blocker selective against peak I_{Na} current and demonstrate the antiarrhythmic and anti-ischemic effects of our clinical candidate molecule **4** (Figure 1) in isolated heart, in vivo S−T ischemia model, and ischemia induced ventricular arrhythmia model. To avoid hERG and β-blockade, we screened a small diverse library of in-house heterocyclic compounds (approximately 800 compounds) without a basic group for their late I_{Na} inhibitory activity using an automatic patch clamp system (h $Na_v1.5$ α-subunit human embryonic kidney cell, HEK-293, Q-Patch system). The ensuing hit-to-lead effort resulted in discovery of triazolopyridine **2** (Figure 1).[10,11] The potent late I_{Na} current inhibitor **2** (GS-458967,[10,11] IC_{50} of 333 nM) was found to have a good separation of late I_{Na} current inhibition from peak sodium current but did not have a favorable central nervous system (CNS) window due to high brain penetration and high activity at brain sodium isoforms ($Na_v1.1$, 1.2, 1.3).[10,11] We subsequently discovered **3** (GS-462808,[12,13] Figure 1), with an increased polar surface area from 50 to 84 Å by adding a carbonyl to the core that helped lower the brain penetration and serendipitously decreased activity at the brain sodium isoforms resulting in a more favorable CNS window (20-fold).[12,13] Unfortunately, **3** was found to have a metabolic liability, leading to liver lesions in 7 day rat toxicology studies that may be due to oxadiazole cleavage or glutathione addition to the core.[12,13] We will describe the SAR leading to the discovery of 3,4-dihydrobenz-[*f*][1,4]oxazepin-5(2*H*)-one **4** (GS-6615,[14,15] Figure 1) and its improved properties relative to **1**.[14,15]

RESULTS

Chemistry. The general route to all of the late I_{Na} inhibitors in this article utilized an alkylation step of the amide nitrogen

Scheme 1. Preparation of Benzotriazinone 15[a]

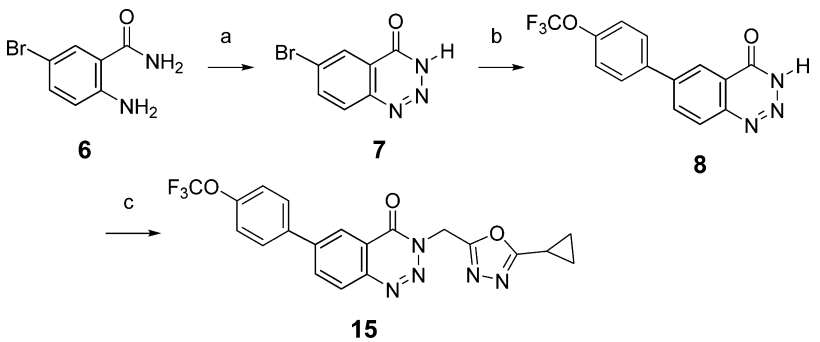

[a]Reagents and conditions: (a) NaN_3, 2N aq HCl; (b) 4-$CF_3OC_6H_4B(OH)_2$, $Pd(dppf)Cl_2 \cdot CH_2Cl_2$, K_2CO_3, toluene/*i*-PrOH/H_2O; (c) 3-(chloromethyl)-5-cyclopropyl-1,3,4-oxadiazole, DMF, K_2CO_3, Et_3N.

DOI: 10.1021/acs.jmedchem.6b00939
J. Med. Chem. XXXX, XXX, XXX−XXX

and a palladium mediated Suzuki−Miyaura coupling, as illustrated in Scheme 1 for compound **15**. The benzotriazinone synthesis commenced with commercially available compound **6** (Scheme 1).[16] Diazotization and in situ ring closure to the benzotriazinone core was invoked by treatment with sodium nitrite and hydrochloric acid. The 5-bromoquinazolin-4(3*H*)-one and 5-bromophthalazin-1(2*H*)-one cores were prepared from commercial starting materials (Scheme 2). The lactam

Scheme 2. Preparation of Quinazolin-4(3*H*)-one and Phthalazin-1(2*H*)-one Derivatives[a]

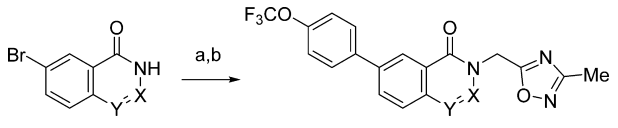

16 X = CH, Y = N
17 X = N, Y = CH

[a](a) $R^1PhB(OH)_2$, $Pd(dppf)Cl_2{\cdot}CH_2Cl_2$, $NaHCO_3$, DMF; (b) R^2-X, X = Cl or Br, NaH, DMF, 80 °C, 24 h.

core was prepared by a Beckmann rearrangement initiated by treatment with sodium azide and methanesulfonic acid (Scheme 3).[16] 3,4-Dihydrobenzo[*f*][1,4]oxazepin-5(2*H*)-one core commenced with commercially available 6-bromochroman-4-one that underwent ring expansion by Beckmann rearrangement. The order of Suzuki−Miyaura coupling and *N*-alkylation is interchangeable and depended on the focus of the SAR effort (routes 1 and 2, Scheme 4).

Initially, we stayed close to the [1,2,4]triazolo[4,3-*a*]pyridin-3(2*H*)-one core of **3** by adding another nitrogen to make the 6,6-benzo[*d*][1,2,3]triazin-4(3*H*)-one core of **15**, but we replaced the 3-methyl-1,2,4-oxadiazol-5-yl)methyl D-ring of **3** with a less metabolic labile 5-cyclopropyl-1,3,4-oxadiazol-2-yl)methyl D-ring (Scheme 1). Compound **15** retained the high polar surface area of 84 Å, had a lower brain to plasma ratio than **3** (0.84 versus 1.5), and demonstrated anti-ischemic activity in vivo with an EC_{50} of 970 nM in the rabbit S−T model (Table 1).[16] The benzotriazinone series had a number of highly active compounds in the rabbit S−T model and the lowest brain to plasma ratios as a class. However, we were not comfortable developing a compound from the benzotriazinone class due to the lack of precedence in pharmaceutical development and the inherent low solubility (1−4 μM). We tried removing a nitrogen to the more generally accepted quinazolin-4(3*H*)-one **16** and phthalazin-1(2*H*)-one **17** (Scheme 2) that retained inhibition of late I_{Na} current, but unfortunately this resulted in much higher brain to plasma ratios 15.0 and 4.4, respectively.

To enhance water solubility for potential use as an intravenous agent, we tried to break the planarity of the unsaturated ring system and switch to a partially saturated 6,6 lactam system exemplified by **18** and **19** (Table 2) and that did indeed result in improved water solubility to 28 and 60 μM, respectively, and retained inhibition of late I_{Na} current in cells. Both compounds had good metabolic stability, but neither compound was very active in reversing the effects of ATX-II induced late I_{Na} on monophasic action potential $duration_{90}$ ($MAPD_{90}$) in isolated hearts (IH assay described in detail below). The addition of an oxygen and expanding to a seven-membered 3,4-dihydrobenzo[1,4]oxazepinone ring as in compounds **20** and **4** resulted in retaining good solubility and inhibition of late I_{Na} current both in cells and isolated heart preparations (62% reversal at 1 μM). It appears that the late I_{Na} inhibitor pharmacophore prefers a H-bond acceptor at this position consistent with series like the 3,4-dihydrobenzo[1,4]-oxazepinone, providing good activity in isolated heart and downstream anti-ischemic assays (rabbit S−T). Both **20** and **4** had a 10-fold separation of inhibition of late I_{Na} current in cells at the cardiac $Na_v1.5$ channel from the inhibition of high frequency 25 Hz (Hz) brain isoform $Na_v1.1$. Compound **4** with the 4-trifluoromethoxyphenyl had better human microsomal metabolic stability than the 4-trifluoromethylphenyl analogue **20**, and it became the development compound based on this stability and subsequent activities in downstream assays (e.g., rabbit ΔS−T).

We next explored ring C SAR to determine whether the 4-trifluoromethoxyphenyl substituent of **4** was optimal. The 3-trifluoromethoxyphenyl analogue **21** has less late I_{Na} inhibition (2×), is less metabolically stable in human microsomes, and is less active in reversing the effects of ATX-II induced late I_{Na} $MAPD_{90}$ in isolated hearts (Table 3). The 2- trifluoromethoxyphenyl analogue **22** is much less active in late I_{Na} inhibition relative to the 4-trifluoromethoxyphenyl of **4**. Similarly, the 3-trifluoromethylphenyl analogue **23** has less late I_{Na} inhibition (3×) than the 4-trifluoromethylphenyl **20**. The 4-chlorophenyl derivative **24** has less late I_{Na} inhibition (2×) than **4**, and it was less metabolically stable in human microsomes. The importance of the electronic and lipophilic effect of the 4-trifluoromethoxyphenyl of **4** can be noted when comparing late I_{Na} inhibitory activity for the 4-methoxyphenyl analogue **25** and the unsubstituted derivative **26** that were found to be much less active (clogD of **4** is 3.56 vs 3.01 for **25**). The CF_3O- group has been referred to as a pseudohalogen with a Pauling electronegativity of 3.7 that lies between F −4.0 and Cl −3.0, and it is quite lipophilic with a π of 1.04.[17] The CH_3O- is much less electron withdrawing, having a Pauling electronegativity of 2.7 (closer to Br −2.8) with a π of −0.02.[17] In addition, the conformation of the two groups are different based on analysis of Cambridge Crystallographic Database data, CH_3O- carbon typically lies within the plane of the phenyl, but the CF_3O- carbon lies closer to 90° out of plane.[18] This was confirmed by single crystal X-ray for **4**, where the carbon of the

Scheme 3. Preparation of Lactam Core Derivatives[a]

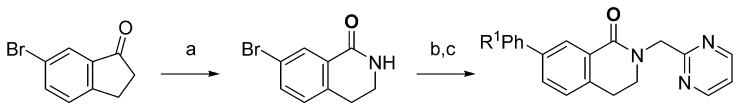

9 **10** **18 - 19**

[a]Reagents and conditions: (a) NaN_3, $MeSO_3H$, 0 °C; (b) $R^1PhB(OH)_2$, $Pd(dppf)Cl_2{\cdot}CH_2Cl_2$, $NaHCO_3$, DMF; (c) R^2-X, X = Cl or Br, NaH, DMF, 80 °C, 24 h.

DOI: 10.1021/acs.jmedchem.6b00939
J. Med. Chem. XXXX, XXX, XXX−XXX

Scheme 4. Preparation of 3,4-Dihydrobenzo[*f*][1,4]oxazepin-5(2*H*)-one Derivatives[a]

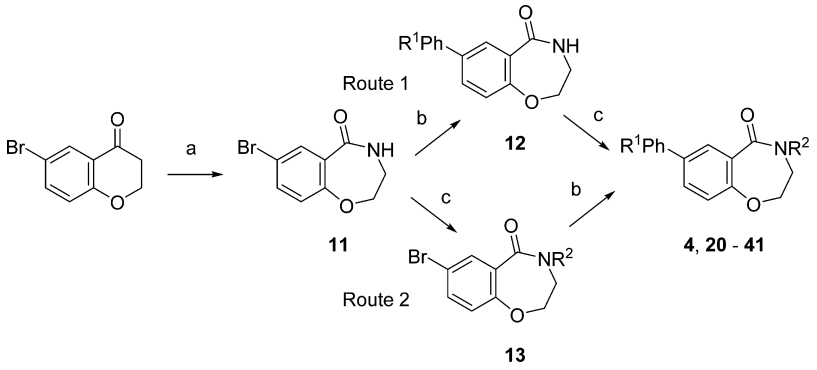

[a]Reagents and conditions: (a) NaN_3, $MeSO_3H$, 0 °C; (b) $R^1PhB(OH)_2$, $Pd(dppf)Cl_2{\cdot}CH_2Cl_2$, $NaHCO_3$, DMF; (c) R^2-X, X = Cl or Br, NaH, DMF, 80 °C, 24 h.

Table 1. Fused Rings Comparison: Benzo[*d*][1,2,3]triazin-4(3*H*)-one, Quinazolin-4(3*H*)-one, and Phthalazin-1(2*H*)-one

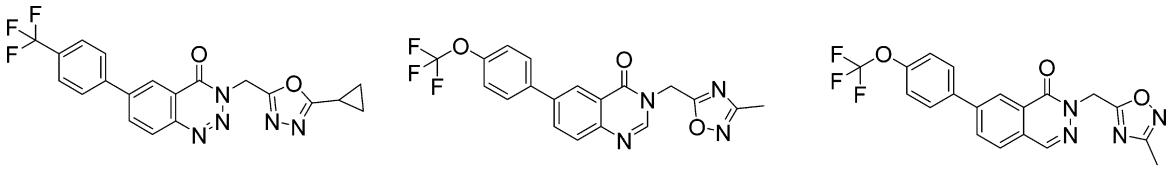

15 **16** **17**

	15	16	17
late I_{Na}, % block at 1 μM	51	48	39
ΔS-T EC_{50}, nM	970		
B:P, fold	0.86	15	4.4
PSA, Å^2	84	80	80

Table 2. Sodium Channel Blocking Properties of Lactam versus 3,4-Dihydrobenzo[1,4]oxazepinone Compounds

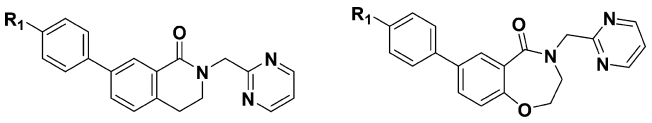

					microsomal $t_{1/2}$, min			
	R^1	late I_{Na} block, IC_{50}, μM	solubility, μM	peak $Na_v1.1$, % block at 10 μM	h	r	d	isolated heart (1 μM), ΔAPD_{90}, %
18	4-CF_3	2.07	28	15	304	354	320	−25
19	4-CF_3O	2.31	60	23	395	150	157	−6
20	4-CF_3	1.08	87	60	348	211	371	−62
4	4-CF_3O	0.88	24	53	395	200	354	−62

CF_3O− group lies on average 83° out of plane of the phenyl ring (Figure 3). The CF_3− group has a comparable Pauling electronegativity of 3.5 to the CF_3O− group, and it is quite lipophilic with a π of 0.88, so it is consistent that **20** would have similar late I_{Na} inhibitory to **4** (cLogD of **20** is 3.37).[17] The 4-CHF_2O− group of **27** imparts a decreased late I_{Na} inhibition that may be imparted due to the decreased lipophilicity (cLogD 3.2) and the conformational effects where the CHF_2O− θ typically lies between 0° and 50°.[18] Also, the 4-CHF_2− group of **28** imparts a decreased late I_{Na} inhibition that may be imparted due to the decreased lipophilicity (**28** cLogD 2.95).[18,19] Highly polar groups such as 4-$MeSO_2$− led to loss of late I_{Na} inhibition for **29** consistent with the phenyl substituent binding in a hydrophobic pocket. The 4-Cl,3-F-phenyl derivative **30** was 2× less active than **4** in cells but retained good late I_{Na} inhibition in the isolated heart assay. Adding an *ortho*-F group (**31**) to **4** led to comparable late I_{Na} inhibition but resulted in lower human microsomal stability. Adding a *meta*-Cl (**32**) to **4** led to good activity, retention of metabolic stability, but decreased activity in ex vivo assay (IH). As expected, the addition of a 2-acetamido group to **4** affording **33** resulted in a considerable loss of late I_{Na} inhibition. The 4-trifluoromethoxyphenyl group of **4** provided the best overall properties, so this was fixed and we explored the D ring SAR (Table 4). Prior to changing the D ring, we checked the linker length. We found that longer linkers led to a loss in metabolic stability as exemplified by the ethyl linker **34** (propyl was also less stable, not shown). The pyridyl D ring analogue **35** (a one nitrogen change from **4**), resulted in retaining late I_{Na} inhibition, a slight increase in peak sodium inhibition, and a decrease in metabolic stability. Addition of a 5-trifluoromethyl to **35** afforded **36** with improved metabolic stability, but the solubility decreased below 1 μM. Replacing the 5-trifluoromethyl group with 5-fluoro **37** resulted in a very potent late I_{Na} inhibitor, but the inhibition of peak $Na_v1.1$ was too high and the metabolic stability decreased substantially. The addition of a

DOI: 10.1021/acs.jmedchem.6b00939
J. Med. Chem. XXXX, XXX, XXX−XXX

Table 3. Sodium Channel Blocking Properties of 3,4-Dihydrobenzo[*f*][1,4]oxazepin-5(2*H*)-one Compounds

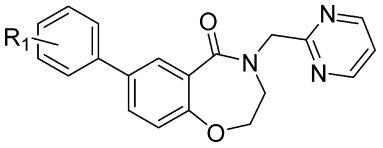

	R[1]	late I_{Na} block, IC_{50} (or % at 1 μM)	peak $Na_v1.5$ block, % (at conc, μM), 3 Hz	peak $Na_v1.1$, % block at 10 μM, 25 Hz	microsomal $t_{1/2}$, min			isolated heart (1 μM) ΔAPD_{90}, %
					h	r	d	
4[b]	4-CF_3O	0.88	24 (3)	53	395	200	354	−62
20[a,b]	4-CF_3	1.08	27 (3)	60	348	211	371	−62
21[b]	3-CF_3O	2.03	3 (3)	18	297	294	43	−29
22[b]	2-CF_3O	(26)						
23[b]	3-CF_3	3.03						
24[b]	4-Cl	1.62	17 (3)	31	194	96	63	−68
25[b]	4-MeO	(13)						
26[b]	H	(18)						
27[b]	4-CHF_2O	(13)						
28[b]	4-CHF_2	(17)						
29[b]	4-$MeSO_2$	(3)						
30[b]	4-Cl,3-F	1.61	8 (1)	23	330	98	115	−58
31[b]	4-CF_3O,2-F	1.28	37 (3)	35	241	308	156	−39
32[b]	4-CF_3O,3-Cl	0.77	15 (3)	33	393	338	NT[c]	−23
33[b]	4-CF_3O,2-MeCONH	(4)						

[a]Prepared by route 1, Scheme 4. [b]Prepared by route 2, Scheme 4. [c]NT = not tested.

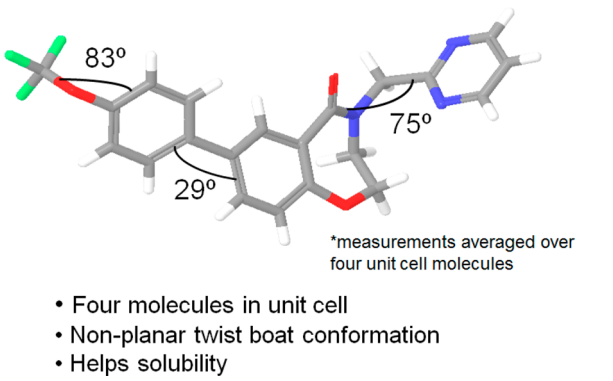

Figure 3. Single crystal X-ray of **4**.

3-methoxy **38** or 3-amino **39** to the D ring led to an increase in the inhibition of peak $Na_v1.1$. A highly polar group with H bond donors was not well tolerated on the D ring (**40**). The compounds of Table 2 and 3 begin to illustrate how challenging it is to optimize all the properties of late I_{Na} inhibitors. The original 4-trifluoromethoxyphenyl C ring and unsubstituted pyrimidine D ring of **4** turned out to be optimal.

A homology model of $Na_v1.5$ was built based on the crystal structure of a bacterial voltage-gated sodium channel, NavAb (3RVY, see Supporting Information).[20] The model was manipulated into several states, including the closed, open, and inactivated states. The closed state differs from the open and inactivated states by a translational motion of the S4 helices in response to voltage changes. The shift in the S4 helices alters the position of the S4−S5 linkers, which constrain the extent of the pore aperture opening formed by the S6 helices.[21] The open and inactivated states differ by a conformational change in the inactivation gate connecting domains III and IV. In the inactivated state, the inactivation gate closes over the channel opening, directing the residues I1485, F1486, and M1487 into the hydrophobic pore.[22] Various compounds described here were docked into the three states of the channel, and a consensus binding mode emerged for compounds docked to the open and inactivated states. This binding mode, as illustrated in Figure 4 for compound **4**, suggests compounds rest in the lidocaine pocket, with the biphenyl motif forming stacking interactions with F1760 and Y1767 on the S6 helix of domain IV. In support of this binding pose, **4** lost late I_{Na} inhibition with the mutants F1760A or Y1767A in a similar manner to **1**. The trifluoromethoxy group of compound **4** is positioned toward the hydrophobic opening of the channel, interacting primarily with I1466 on the S6 helix of domain III and I1768 on the S6 helix of domain IV. An interaction with F1486 of the inactivation gate may also be possible in the inactivated state. The more polar end of the molecule is directed toward the selectivity filter, defined by the residues D372, E898, K1419, and A1711.[23]

Next, we evaluated the antiarrhythmic and anti-ischemic effects of **4** versus **1** in isolated heart, in vivo ischemia model (rabbit ΔS−T), and ischemia induced ventricular arrhythmia model. Late I_{Na} was induced in ex vivo isolated rabbit hearts through the addition of toxin ATX-II that prolongs the $MAPD_{90}$ by approximately 100 ms (ms, Figure 5). Late I_{Na} inhibitors **4** or **1** reverse the prolongation of $MAPD_{90}$ in the isolated heart but to a different degree and potency. Compound **4** reverses the ATX-II effect by 100% with an IC_{50} of 700 nM, while **1** provides only a partial reversal by 60% with an IC_{50} of 16 μM. Compound **4** is 22 times more potent in reversal of late I_{Na} effects than **1**. It is noteworthy that neither **4** or **1** have L-type calcium channel activity at the concentrations tested as this would also shorten the $MAPD_{90}$. The prolongation of $MAPD_{90}$ by late I_{Na} translates into a longer QT interval in vivo. In these isolated heart ex vivo studies, the effect of **4** is much more pronounced on the QT interval with complete reversal of ATX-

DOI: 10.1021/acs.jmedchem.6b00939
J. Med. Chem. XXXX, XXX, XXX−XXX

Table 4. Sodium Channel Blocking Properties of 3,4-Dihydrobenzo[*f*][1,4]oxazepin-5(2*H*)-one Compounds[a]

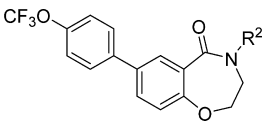

	R^2	Late I_{Na} block, IC_{50} (or % at 1 μM)	peak $Na_v1.5$ block, % (at conc., μM), 3 Hz	peak $Na_v1.1$, % block at 10 μM, 25 Hz	Microsomal $t_{1/2}$, min		
					h	r	d
4	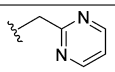	0.88	24 (3)	53	395	200	354
34	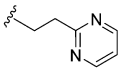	1.00	13 (3)	67	28	28	93
35	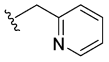	0.50	22(1)	67	150	69	167
36	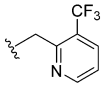	0.85	13 (1)	40	395	188	395
37	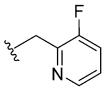	0.16	23(0.3)	82	149	89	194
38	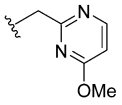	0.97	27 (1)	60	395	271	87
39	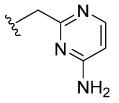	2.48	37(3)	52	NT[b]	NT[b]	NT[b]
40	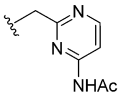	(6)					

[a]All compounds in this table were prepared by route 1, Scheme 4. [b]NT = not tested.

II induced prolongation as compared to a partial reversal observed with **1** (Figure 5). Patients with long QT-3 have a persistent current late in the action potential duration due to mutations in their sodium channel that lead to improper inactivation of the channel. Both **1** and **4** have been shown to shorten the long QT interval in LQT-3 patients that is consistent with late I_{Na} inhibition.[24,25] The ATX-II isolated heart model is an ex vivo LQT3 model. Compound **1** has been shown in chronic angina patients to increase their treadmill exercise times before angina pain develops that correlates with changes in their S−T segment during exercise.[7] Preclinically, **1** inhibits the S−T segment elevation with an EC_{50} of 8 μM in a rabbit model of ischemia where the LAD artery of a rabbit heart is occluded for 15 min and **1** was infused prior to ischemia (Figure 6). Compound **4** inhibits S−T segment elevation with an EC_{50} of 190 nM, and it nearly abolishes S−T segment elevation at 500 nM (93% inhibition). Compound **1** only inhibits 60% of S−T segment elevation at 12 μM. Compound **20** inhibits S−T elevation with an EC_{50} of 300 nM, slightly inferior to **4**. The favorable activity of **4** in the rabbit S−T assay is even more than expected based on cellular late I_{Na} inhibition (IC_{50} = 600 nM, −120 mV, manual patch HEK-293). Compound **4** has increased late I_{Na} potency, as the resting membrane voltage decreases to −80 mV with an improvement in IC_{50} to 100 nM. This enhanced voltage dependent block (VDB) of **4** for late I_{Na} current is consistent with ischemic states where resting membrane potentials are as low as −75 mV. Previously, Pierre Fabre researchers found their lead late I_{Na} inhibitors that performed well in advanced ischemia models had a high degree of VDB.[26,27] While the VDB IC_{50} is more in line with the rabbit S−T EC_{50}, we did check all off target cardiac ion channels that would affect efficacy and a full selectivity panel of receptors where **4** was completely clean of effects at 1 μM (see Supporting Information, Table 1). The improved efficacy (93%) and potency (42 times) of **4** relative to **1** in the rabbit S−T model prompted our decision to advance **4** to development. We wanted to evaluate additional indications for **4** and turned to an ischemia induced ventricular arrhythmia model (Figure 7). In the VT−VF model, we constrict the left circumflex artery in the rabbit for 30 min to

DOI: 10.1021/acs.jmedchem.6b00939
J. Med. Chem. XXXX, XXX, XXX−XXX

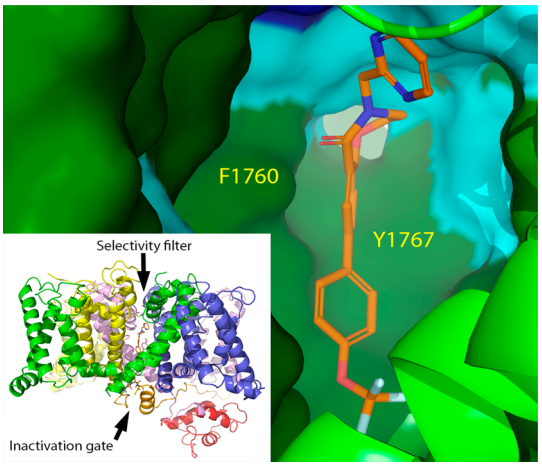

Figure 4. Homology model of compound **4** bound to the inactivated state of $Na_v1.5$. Protein surface is colored by residue type: green is hydrophobic, cyan is polar, blue is positively charged. The compound is suggested to bind with its biphenyl motif sandwiched between F1760 and Y1767, which define the lidocaine pocket. Its hydrophobic end (trifluoromethoxy) is directed toward the inactivation gate, while its polar end (pyrimidine) is directed toward the selectivity filter. Inset shows the full length model. Domain I is blue, domain II is green, domain III is yellow, and domain IV is pink. The inactivation gate linking domains III and IV is orange. The C-terminus is red. Compound **4** is seen to bind in the channel pore.

induce the control animals to have episodes of VT and VF. Both the class Ic peak sodium current inhibitor flecainide and class 1b mexiletine increase ventricular tachycardia/fibrillation (VT−VF) and subsequent death due to their pro-arrhythmic properties (Figure 7 and Supporting Information, Figure 2).[28] Compound **4** (class Ib) completely inhibits VT−VF and death at 2.5 μM with an EC_{50} of approximately 1.7 μM. Previously, we found that **1** was only partially protective in a chemically induced Torsades des Pointes (TdP) assay with 40% of the animals having Tdp at 14 μM.[13] Compound **4** was also evaluated in the chemically induced TdP assay, and it was again completely protective at 2.5 μM (see supplement). Overall, compound **4** had marked improvement in potency and efficacy relative to **1** in animal models of ischemia and arrhythmia consistent with advancement as a second-generation late I_{Na} inhibitor, so we further characterized its ion channel and PK properties.

Our initial triazolopyridine lead **2** has an IC_{50} of 400 nM against the brain sodium isoforms $Na_v1.1$, 1.2, 1.3 with a stimulating frequency of 10 Hz, while **4** has an IC_{50} of 96, 60, and 16 μM, respectively (Table 5).[11] This enhanced selectivity is thought to be important to avoid off-target CNS effects observed with **2** that resulted in a narrow therapeutic index. It is also important to avoid hitting the muscular isoforms $Na_v1.4$ and 1.6 to avoid tremors in the peripheral nervous system where **4** has low activity as well. The $Na_v1.7$ and 1.8 are targets for pain indications in the periphery where the high frequency (25 Hz) inhibition by **4** may actually prove beneficial in diabetic neuropathy, a common co-morbidity of ischemic patients. It is noteworthy that **1** has demonstrated efficacy in preclinical models of pain.[29] Compound **4** has use dependent block with increased activity for late I_{Na} inhibition with an IC_{50} less than 100 nM for 3 Hz stimulation (180 beats per minute). The off-target activity for **4** does increase at the high frequency of 25 Hz, but it is still above 3 μM for the brain isoforms. Ultimately, **4** was found to be well tolerated in vivo as far as a CNS effects with single ascending dose studies in rat and dog supporting adverse events occurring above 10 μM. Compound **4** was found to be approximately 10 times more potent than **1** for late I_{Na} inhibition in cells (Table 6) while maintaining a good separation from peak sodium inhibition. Compound **1** has only a 2 fold separation of late I_{Na} inhibition from hERG inhibition, but **4** has a 10-fold separation. The late I_{Na} inhibiting effects of **1** on $MAPD_{90}$ in isolated hearts are likely compromised by its hERG inhibition that works against it. This may be the reason for the partial efficacy observed with **1** in the isolated heart assay. Both **4** and **1** have low activity at the brain isoform $Na_v1.1$ at 10 μM with 10 Hz stimulation.

We evaluated the pharmacokinetics of **4** across species with a good correlation between in vitro and in vivo clearance in rat and dog but a slightly lower clearance (3×) observed in vivo in the cynomolgus monkey (Table 7). The volume steady state (V_{ss}) across species was in an acceptable range where allometric scaling projected a human volume of 1.5 L/kg. The half-life of **4** varied from 5 h in the cyno to 27.9 h in dog. Compound **4** had

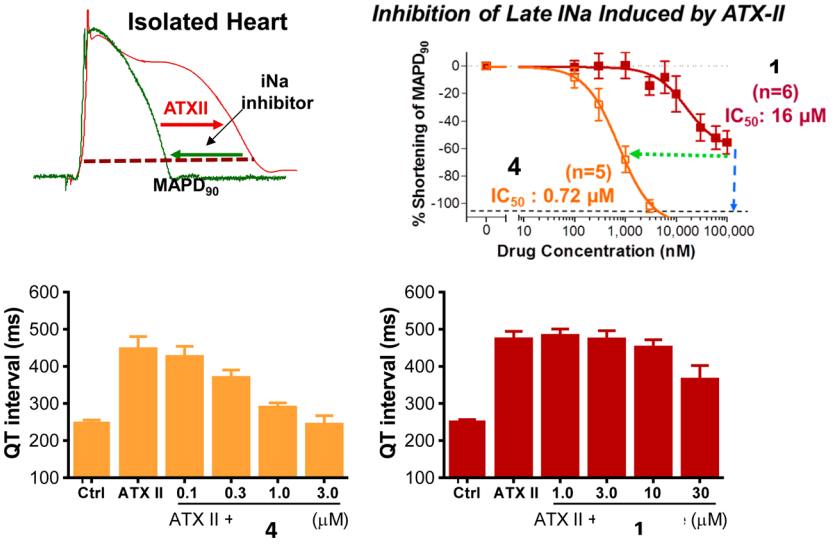

Figure 5. LQT-3 model **4** (orange) vs **1** (red), ex vivo isolated heart IC_{50} (rabbit).

DOI: 10.1021/acs.jmedchem.6b00939
J. Med. Chem. XXXX, XXX, XXX−XXX

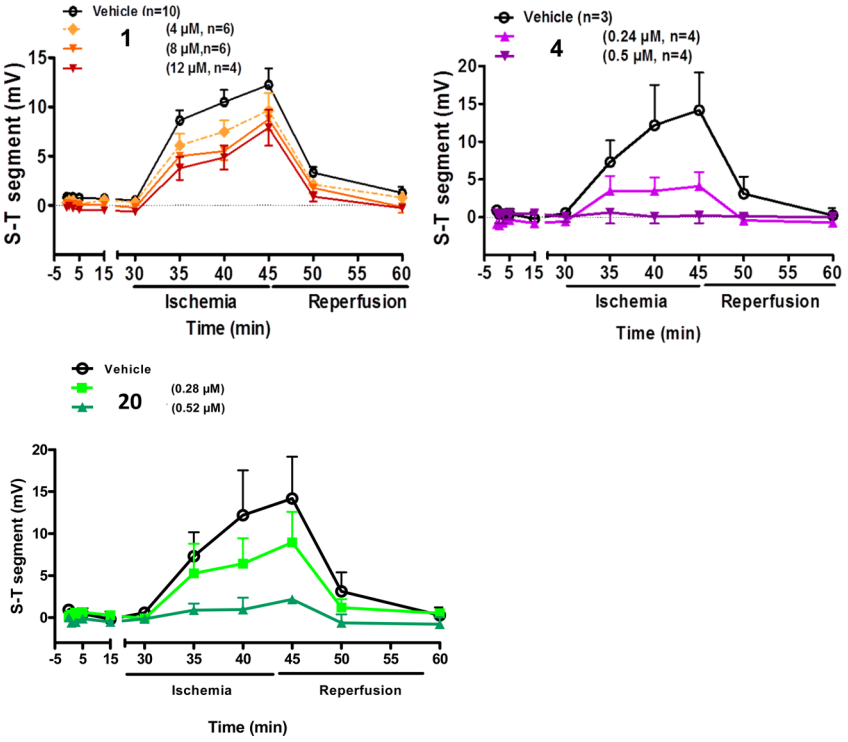

Figure 6. Anti-ischemic effect of **1** versus **4** versus **20** in left anterior descending (LAD) coronary occlusion model (15 min, rabbit).

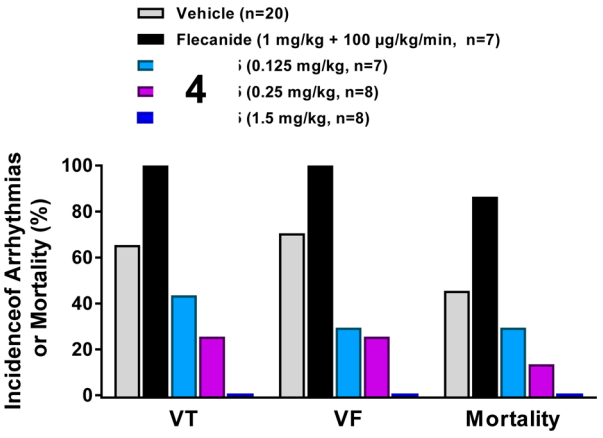

Figure 7. **4** suppresses ischemia induced VT−VF arrhythmias recorded during 30 min of LCX ligation in anesthetized rabbits. Flecainide (class 1c antiarrhythmic) and mexiletine (class 1b antiarrhythmic, Supporting Information, Figure 2) induce VT−VF and mortality at clinical exposures.

Table 5. Sodium Channel Blocking Properties of 3,4-Dihydrobenzo[*f*][1,4]oxazepin-5(2*H*)-one 4 (Manual Patch Clamp)

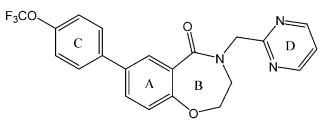

4 GS-6615

$Na_v1.5$ - Late I_{Na}

0.1 Hz - 0.60 μM

1 Hz - 0.26 μM

3 Hz - <0.1 μM

Na^+ channel isoform	IC_{50} (μM) stimulating frequency (Hz)	
	10 Hz	25 Hz
$Na_v1.1$	~96	3.4
$Na_v1.2$	~60	10
$Na_v1.3$	~16	3.5
$Na_v1.4$	~13	3.3
$Na_v1.6$	~28	4
$Na_v1.7$	5	1
$Na_v1.8$	~18.8	1.5

Table 6. Sodium Channel Blocking Properties of 3,4-Dihydrobenzo[*f*][1,4]oxazepin-5(2*H*)-one 4 versus 1 (Manual Patch Clamp)

	4	1
late I_{Na} IC_{50} (μM) ATX II	0.62 (10-fold)	6.9
peak I_{Na} IC_{50} (μM) (peak/late)	51 (82-fold)	428 (62-fold)
hERG IC_{50} (μM) (hERG/late)	6.0 (10-fold)	12 (2-fold)
peak $Na_v1.1$ @ 10 μM (10 Hz)	no effect	no effect

good oral bioavailability across species consistent with excellent permeability (heterogeneous human epithelial colorectal adenocarcinoma, CACO-2 A → B/B → A 34.6/29 × 10^{-6} cm/s) and low first-pass metabolism. The low clearance in pooled human hepatocytes using tritiated **4** was consistent with once a day dosing. The subsequent maintenance doses of **4** used in phase II trials were 3 and 6 mg per day.[25] We do not anticipate drug−drug interactions with **4** as there were no significant inhibitory activity observed against the major cytochrome P450s (>10 μM, Cyp 3A4, 2D6, 2C8, 1A, 2C9, 2C19, 2B6). We did measure the levels of **4** in the brain in the rat after oral dosing, and the total brain to plasma ratios were approximately 3:1. Fortunately, **4** was found to be well tolerated in vivo in the rat as far as a CNS effects due to the decreased activity at the brain isoforms as mentioned above.

DOI: 10.1021/acs.jmedchem.6b00939
J. Med. Chem. XXXX, XXX, XXX−XXX

Table 7. Preclinical PK Properties across Species for 4

	parameter	SD rat	beagle dog	cyno monkey	human
hepatocytes ^{3}H-**4**	Cl_{int} (L/h/kg)	0.16	0.06	0.36	<0.015
IV	Cl (L/h/kg)	0.14	0.042	0.11	
	V_{ss} (L/kg)	2.5	1.6	1.5	
	$T_{1/2}$ (h)	13	27.9	5.0	
PO	%*F*	91	100	39	

CONCLUSION

We identified **4** as an appropriate second-generation late I_{Na} inhibitor with improved potency and efficacy relative to **1** in cells, ex vivo isolated hearts, and in animal models of ischemia and arrhythmia. Late sodium current is enhanced during ischemia, leading to calcium overload that increases energy demand during ischemia and increases the probability of early after depolarizations and delayed after depolarizations, both triggers for arrhythmias.[4] The first-generation late I_{Na} inhibitor **1** within its therapeutic range (2−8 μM) does not completely inhibit late I_{Na} (estimated at 15−30% inhibition based on rabbit S−T), has only a 2-fold selectivity over hERG, has significant β-blocker activity at therapeutic concentrations, requires twice a day dosing at approved doses up to 1000 mg, and has dizziness as a side effect due to CNS effects (6% at 1000 mg). Compound **4** is estimated to have a 100% coverage of late I_{Na} inhibition at 1 μM (based on rabbit S−T), has a 10-fold selectivity over hERG, does not inhibit β-receptors at 10 μM, is QD at 3 and 6 mg, and was well tolerated in phase I studies. Compound **4** is 10 times more potent late I_{Na} inhibitor than **1** in cells and 22 times more potent in isolated heart ex vivo assay. Compound **4** was 42 times more potent than **1** in reducing ischemic burden in vivo (rabbit S−T segment) with 93% inhibition at 500 nM, while **1** provided only 60% at 12 μM. In a drug-induced model of *TdP* ventricular arrhythmia model (supplement), **4** was completely protective at 2.4 μM, while **1** provides only 60% reduction at 14 μM. Compound **4** does not potentiate ischemia-induced arrhythmias (VT−VF) or mortality as was observed with other class 1 antiarrhythmics in the LCX model. Compound **4** is currently in clinical development for treatment of LQT-3 syndrome, HCM, and VT−VF. Compound **4** represents a new class of potent late I_{Na} inhibitors that will be useful in further delineating the role of inhibitors of this current in the treatment of patients with cardiovascular disease.

EXPERIMENTAL SECTION

Nuclear magnetic resonance (NMR) spectra were recorded on Varian Mercury Plus 400 MHz and a Varian Unity Plus 500 MHz spectrometers at room temperature, with tetramethylsilane as an internal standard. Chemical shifts (δ) are reported in parts per million (ppm), and signals are reported as s (singlet), d (doublet), t (triplet), q (quartet), m (multiplet), or br s (broad singlet). Purities of the final compounds were determined by HPLC and were greater than 95%. HPLC conditions to assess purity were as follows: Agilent HPLC, Phenomenex Kinetix C18, 4.6 mm × 100 mm (2.6 μm); gradient of 0.1% TFA water (A) and 0.1% TFA acetonitrile (B) start at 98:2 A:B with 8.5 min gradient to 0:100; flow rate, 1.5 mL/min; wavelength, UV 254 nM. The LC-MS spectra were obtained on an Agilent system with the following HPLC conditions: column, Phenomenex Luna C18, 4.6 mm × 75 mm (5 μm), gradient of 0.05% TFA water (A) and 0.04% TFA acetonitrile (B), flow rate, 1.0 mL/min. The preparative HPLC system includes two sets of Gilson 332 pumps, a Gilson 156 UV/vis detector, and a Gilson 215 injector and fraction collector, with Trilution LC software. A Phenomenex Luna 150 mm × 21.2 mm column was used. The mobile phase was a gradient of 0.1% TFA water (A) and 0.1% TFA acetonitrile (B). High-resolution mass spectra were recorded on a Xevo G2 Q−T of mass spectrometer with an ESI source.

7-(4-(Trifluoromethoxy)phenyl)-3,4-dihydrobenzo[*f*][1,4]-oxazepin-5(2*H*)-one (4). Commercially available 6-bromochroman-4-one (1.0 g, 3 mmol) was dissolved in 10 mL of methanesulfonic acid. The solution was cooled using an ice bath, and sodium azide (0.30 g, 4.5 mmol) was added over a period of 45 min. The mixture was stirred at RT for 16 h. The mixture was neutralized using conc HCl. The resulting solid was filtered and washed with water to afford **11** as analytically pure sample.

Route 2: To a solution of **11** (20.0 g, 0.083 mol, 1 equiv) and 2-(chloromethyl)pyrimidine (25.0 g, 0.15 mol, 1.8 equiv) in DMF (150 mL), NaOH solution (20 mL, 10M, 5 equiv) was slowly added at room temperature (slightly exothermic) and stirred at rt for 10 min, followed by heating at 95 °C for 2 h. After cooling the reaction mixture, ethyl acetate (200 mL) was added and the organic layer was separated. The organic layer was washed with water (20 mL), brine, dried over sodium sulfate, and concentrated. The residue was dissolved in 1,4-dioxane (50 mL) and to this 4 N HCl in dioxane (50 mL) and conc HCl (2 mL) was added and stirred at room temperature for 4 h. The resulting precipitate was filtered, washed with ethyl acetate, and dried. Compound **13** obtained (30 g, 98.0%) was obtained as a light-yellow solid. To the bromide **13** (15 g, 0.04 mol, 1 equiv), 4-trifluoromethoxyphenylboronic acid (12.5 g, 0.06 mol, 1.5 equiv) and potassium carbonate (22.0 g, 0.16 mol, 4 equiv) in a round-bottom flask, solvent (150 mL, toluene/2-propanol/water, 2/1/1) was added and stirred under nitrogen for 10 min. To the above solution, the palladium catalyst Pd(dppf)Cl_2·CH_2Cl_2 (1.0 g, 0.012 mol, 0.02 equiv) was added and heated at 85 °C for 2 h. The reaction mixture was diluted with ethyl acetate (300 mL), and the organic layer was separated, filtered through a plug of Celite and silica gel, and concentrated in vacuo. Flash column purification on silica gel using ethyl acetate/hexane as eluent provided **4** (13.0 g 78%). This reaction was repeated to afford an additional 13.0 g of **4**. To a solution of **4** (26 g) in 1,4-dioxane (25 mL), 4 N HCl/dioxane (25 mL) was added followed by conc. HCl (2 mL) and stirred at room temperature for 4 h. Solvent was distilled off, and dichloromethane was added and distilled off. To the residue, ethyl acetate (150 mL) was added and stirred at room temperature overnight. The precipitate was filtered, washed with ethyl acetate and hexane, and dried under vacuum. Compound **4 HCl** obtained (24.8 g) was obtained as a white solid. Anal. HPLC 100% (6.78 min). ^{1}H NMR ($CDCl_3$) δ 8.72 (d, 2H, *J* = 5.2 Hz), 8.17 (d, 1H, *J* = 2.4 Hz), 7.59−7.63 (m, 3H), 7.26 (d, 2H, *J* = 3.2 Hz), 7.22 (t, 1H, *J* = 4.8 Hz), 7.10 (d, 1H, *J* = 8.4 Hz), 5.10 (s, 2H), 4.56 (t, 2H, *J* = 5.0 Hz), 3.77 (t, 2H, *J* = 5.0 Hz). LCMS *m*/*z* 416.1 (M + H). HRMS-ESI+: $[M + H]^+$ calcd for $C_{21}H_{16}F_3N_3O_3$, 416.1217; found, 416.1215.

6-Bromobenzo[*d*][1,2,3]triazin-4(3*H*)-one (7). To a mixture of commercially available compound **6** (9.250 g, 43.03 mmol) and sodium nitrite (8.909 g, 129.11 mmol) in 1,4-dioxane (40 mL) was added dropwise 2N aqeuous HCl (80 mL, 160.00 mmol) with vigorous stir over a period of 30 min, during which H_2O was added twice (40 mL each at 10th and 20th min). After completion of addition, the reaction mixture was stirred overnight then diluted with H_2O (200 mL), sonicated, filtered, washed with H_2O (500 mL), and dried to afford the desired product as **7**. LCMS *m*/*z* 226.0 (M + H), 228.0 (M + H + 2). Anal. HPLC > 98%. ^{1}H NMR (400 MHz; DMSO-d_6) δ 8.30 (d, *J* = 2.3 Hz, 1H), 8.22 (dd, *J* = 8.6, 2.0 Hz, 1H), 8.10 (d, *J* = 9.0 Hz, 1H).

6-(4-(Trifluoromethoxy)phenyl)benzo[*d*][1,2,3]triazin-4(3*H*)-one (8). To a solution of **7** (1.130 g, 5.0 mmol) and 4-trifluoromethoxyphenylboronic acid (1.544 g, 7.5 mmol) in DMF (30 mL) was added K_2CO_3 (2.073 g, 15.0 mmol) and H_2O (3 mL). The reaction mixture was stirred for 5 min under an atmosphere of dry N_2. Pd(dppf)Cl_2·CH_2Cl_2 (146 mg, 0.20 mmol) was added, and the

DOI: 10.1021/acs.jmedchem.6b00939
J. Med. Chem. XXXX, XXX, XXX−XXX

resulting mixture was heated at 98 °C until **7** was consumed (LCMS). The reaction mixture was cooled, diluted with EtOAc (70 mL), filtered through a layer of Celite, washed with 20% DMF in EtOAc (100 mL), transferred to a separation funnel, organic phase was washed with 0.5 M K_2CO_3 (50 mL, 25.0 mmol), 30% aqeuous NH_4Cl (100 mL)and brine (100 mL), dried, and concentrated. To the crude product was added 10% EtOAc in *n*-hexane (10 mL), sonicated, filtered, and washed with 10% EtOAc in *n*-hexane (20 mL) to afford the desired product as **8**, MS *m*/*z* 308.0 (M + H), HPLC purity >97%. ^{1}H NMR matched the desired product. The combined filtrate was concentrated, subjected to Gilson's reverse-phase preparative HPLC with a gradient 0.1% TFA containing CH_3CN/H_2O (10% to 90%) to afford additional desired product as **8**. LCMS *m*/*z* 308.0 (M + H). Anal. HPLC > 99%. The overall combined yield is 71%. ^{1}H NMR (400 MHz; DMSO-d_6) δ 8.42 (m, 1H), 8.39 (d, *J* = 2.3 Hz, 1H), 8.26 (d, *J* = 8.2 Hz, 1H), 8.00 (m, 2H); 7.52 (d, *J* = 8.2 Hz, 2H). ^{19}F NMR (376 MHz; DMSO-d_6) δ −57.2 (s, 3F).

3-((5-Cyclopropyl-1,3,4-oxadiazol-2-yl)methyl)-6-(4-(trifluoromethyl)phenyl)benzo[*d*][1,2,3]triazin-4(3*H*)-one (15). To a solution of **8** (2.446 g, 7.96 mmol) and 3-(chloromethyl)-5-cyclopropyl-1,3,4-oxadiazole (1.660 g, 10.47 mmol) in DMF (15 mL) in a Biotage microwave tube (20 mL capacity) was added potassium carbonate (1.881 g, 13.61 mmol) and triethyl amine (2 mL) with stirring. The reaction mixture was stirred at room temperature for 5 min and then subjected to microwave heating at 120 °C until **8** was consumed in LCMS. The mixture was cooled, diluted with 20% DMF in EtOAc (50 mL), filtered, and washed with 20% DMF in EtOAc (100 mL). The combined filtrate was concentrated in vacuo, dissolved mostly in dichloromethane (20 mL), and filtered, and the filtrate was subjected to Yamazen chromatography over Universal column, eluted with a gradient EtOAc in *n*-hexane to afford, after drying, **15**. Anal. HPLC 97% (7.19 min). **15** was recrystallized from EtOAc/*n*-hexane and dried to give **15**. ^{1}H NMR (400 MHz, DMSO-d_6) δ 8.57−8.44 (m, 2H), 8.36 (d, *J* = 8.4 Hz, 1H), 8.09 (d, *J* = 8.1 Hz, 2H), 7.88 (d, *J* = 8.2 Hz, 2H), 5.82 (s, 2H), 2.20 (ddd, *J* = 8.4, 4.9, 3.5 Hz, 1H), 1.15−1.02 (m, 2H), 1.02−0.86 (m, 2H). HRMS-ESI+: $[M + H]^+$ calcd for $C_{20}H_{14}F_3N_5O_2$, 414.1172; found, 414.1167.

3-((3-Methyl-1,2,4-oxadiazol-5-yl)methyl)-6-(4-(trifluoromethoxy)phenyl)quinazolin-4(3*H*)-one (16). **16** was prepared using the procedures disclosed herein above with the appropriate starting materials. LC/MS (*m*/*z*): 403.0 (M + H$^+$). Anal. HPLC 100% (7.21 min). ^{1}H NMR (chloroform-*d*) δ 8.50 (d, *J* = 2.2 Hz, 1H), 8.24 (s, 1H), 8.01 (dd, *J* = 8.5, 2.2 Hz, 1H), 7.86 (d, *J* = 8.5 Hz, 1H), 7.69 (d, *J* = 8.7 Hz, 2H), 7.33 (dd, *J* = 8.9, 1.0 Hz, 1H), 5.42 (s, 2H), 2.38 (s, 3H). HRMS-ESI+: $[M + H]^+$ calcd for $C_{19}H_{13}F_3N_4O_3$, 403.1013; found, 403.1010.

2-((3-Methyl-1,2,4-oxadiazol-5-yl)methyl)-7-(4-(trifluoromethoxy)phenyl)phthalazin-1(2*H*)-one (17). A mixture of 7-bromophthalazinone (1.09g, 4.84 mmol), 4-trifluoromethoxyphenyl boronic acid (1.20 g, 5.81 mmol), Pd(dppf)Cl_2·CH_2Cl_2 (177 mg, 0.242 mmol), and potassium carbonate (1.34 g, 9.68 mmol) in degassed toluene (4 mL), degassed water (2 mL), and degassed 2-propanol (2 mL) was heated at 90 °C for 12 h. The layers were separated, the organic layer was concentrated, and the residue was purified by trituration with hexanes/ethyl acetate to provide 7-(4-(trifluoromethoxy)phenyl)phthalazin-1(2*H*)-one as a white powder. LCMS *m*/*z* $C_{15}H_9F_3N_2O_2$, 307.2 (M + 1).

To a mixture of 7-(4-(trifluoromethoxy)phenyl)phthalazin-1(2*H*)-one (50 mg, 0.163 mmol), 5-(chloromethyl)-3-methyl-1,2,4-oxadiazole (47.5 mg, 0.359 mmol), and potassium carbonate (68 mg, 9.68 mmol) was added DMF (1 mL), and the reaction was heated to 80 °C overnight. The reaction was diluted with EtOAC and water, the layers were separated, and the organic layer was concentrated to an oil. The residue was purified by flash chromatography (R_f = 0.32, 1:1 hexanes/ethyl acetate) to afford 2-((3-methyl-1,2,4-oxadiazol-5-yl)methyl)-7-(4-(trifluoromethoxy)phenyl)phthalazin-1(2*H*)-one **17** as a white solid. $C_{19}H_{13}F_3N_4O_3$. LCMS *m*/*z* 403.1 (M + 1). Anal. HPLC 99.6% (7.18 min). ^{1}H NMR (DMSO) δ 8.58 (s, 1H), 8.48 (d, *J* = 2.0 Hz, 1H), 8.34 (dd, *J* = 2.0, 8.4 Hz, 1H), 8.12 (d, *J* = 8.4 Hz, 1H), 7.98−8.02 (m, 2H), 7.54 (d, *J* = 8.0 Hz, 1H), 5.67 (s, 2H), 2.31 (s, 1H). HRMS-ESI+: $[M + H]^+$ calcd for $C_{19}H_{13}F_3N_4O_3$, 403.1013; found, 403.1011.

2-(Pyrimidin-2-ylmethyl)-7-(4-(trifluoromethyl)phenyl)-3,4-dihydroisoquinolin-1(2*H*)-one (18). Compound **18** was prepared using the procedures disclosed in the above scheme using the appropriate starting materials. Anal. HPLC 99.3% (6.84 min). ^{1}H NMR (CD_3OD) δ 8.72 (d, 2H, *J* = 4.8 Hz), 8.22 (d, 1H, *J* = 2.0 Hz), 7.77−7.81 (m, 3H), 7.72 (d, 2H, *J* = 8.0 Hz), 7.39 (d, 1H, *J* = 8.0 Hz), 7.34 (t, 1H, *J* = 5.0 Hz), 5.02 (s, 2H), 3.81 (t, 2H, *J* = 6.4 Hz), 3.14 (t, 2H, *J* = 6.4 Hz). MS *m*/*z* 384.1 (M + H). HRMS-ESI+: $[M + H]^+$ calcd for $C_{21}H_{16}F_3N_3O$, 384.1318; found, 384.1316.

2-(Pyrimidin-2-ylmethyl)-7-(4-(trifluoromethoxy)phenyl)-3,4-dihydroisoquinolin-1(2*H*)-one (19). Compound **19** was prepared using the procedures disclosed in the above scheme using the appropriate starting materials. Anal. HPLC 100% (6.96 min). ^{1}H NMR (DMSO-d_6) δ 8.75 (d, 2H, *J* = 5.2 Hz), 8.17 (d, 1H, *J* = 2.4 Hz), 7.78 (m,3H) 7.35−7.45 (m,4H), 4.93 (s, 1H), 3.74−3.78 (t, 2H),3.07−3.10 (t, 2H). LCMS *m*/*z* 400.1 (M + H).

7-(4-(Trifluoromethyl)phenyl)-3,4-dihydrobenzo[*f*][1,4]-oxazepin-5(2*H*)-one (20). Route 1: 7-Bromo-3,4-dihydrobenzo[*f*]-[1,4]oxazepin-5(2*H*)-one (2.0 g), 4-trifluoromethoxyphenylboronic acid (2.2 g), and potassium carbonate (2.0 g) were combined in a mixture of toluene (20 mL), 2-propanol (10 mL), and water (10 mL), and the resulting suspension was degassed with nitrogen. Palladium catalyst Pd(dppf)Cl_2·CH_2Cl_2 was added (0.42 g), and the reaction was heated overnight at 85 °C. After cooling, the aqueous layer was discarded and the organic layer was diluted 2-fold with ethyl acetate, dried over $MgSO_4$, and concentrated. Recrystallization was conducted by dissolving in a minimum necessary amount of dichloromethane and triturating with excess hexane, resulting in 7-(4-(trifluoromethyl)-phenyl)-3,4-dihydrobenzo[*f*][1,4]oxazepin-5(2*H*)-one as a gray solid (1.43 g). ^{1}H NMR: 8.42 (t, 1H), 8.12 (d, 1H), 7.86−7.76 (m, 5H), 7.13 (d, 1H), 4.38 (t, 2H), 3.37 (quartet, 2H). **20** was made via alkylation with 2-(chloromethyl)pyrimidine using the conditions described above for making **13**. Anal. HPLC 100% (6.78 min).

Route 2: To the bromide **13** (28.0 g, 0.083 mol, 1 equiv), 4-trifluoromethylphenylboronic acid (24.0 g, 0.125 mol, 1.5 equiv), and potassium carbonate (45.0 g, 0.332 mol, 4 equiv) in a round-bottom flask, solvent (200 mL, toluene/2-propanol/water, 2/1/1) was added and stirred under nitrogen for 10 min. To the above solution, the palladium catalyst Pd(dppf)Cl_2·CH_2Cl_2 (1.4 g, 0.00166 mol, 0.02 equiv) was added and heated at 85 °C for 3 h. The reaction mixture was diluted with ethyl acetate (200 mL), separated the organic layer, washed with water, and brine. The organic layer was filtered through a plug of Celite and concentrated. Column purification on silica gel using ethyl acetate/hexane (70/30) as eluent provided the product **20** (28.9 g; 87%). ^{1}H NMR ($CDCl_3$) δ 8.80 (d, 2H, *J* = 5.2 Hz), 8.19 (d, 1H, *J* = 2.8 Hz), 7.66−7.71 (m, 5H), 7.33 (t, 1H, *J* = 5.0 Hz), 7.13 (d, 1H, *J* = 8.4 Hz), 5.14 (s, 2H), 4.59 (t, 2H, *J* = 4.8 Hz), 3.81 (t, 2H, *J* = 5.0 Hz). LCMS *m*/*z* 400.1 (M + H). HRMS-ESI+: $[M + H]^+$ calcd for $C_{21}H_{16}F_3N_3O_2$, 400.1267; found, 400.1267.

7-(3-(Trifluoromethoxy)phenyl)-3,4-dihydrobenzo[*f*][1,4]-oxazepin-5(2*H*)-one (21). Compound **21** was prepared according to **4** disclosed herein using the appropriate starting materials. Anal. HPLC 100% (6.86 min). ^{1}H NMR (400 MHz, DMSO-d_6) δ 8.77 (d, *J* = 4.8 Hz, 2H), 8.01 (d, *J* = 2.5 Hz, 1H), 7.81 (dd, *J* = 8.8, 2.4 Hz, 1H)7.77−7.65 (m, 1H), 7.66−7.53 (m, 2H), 7.43 (t, *J* = 4.9 Hz, 1H), 7.36 (d, *J* = 8.2 Hz, 1H), 7.17 (d, *J* = 8.5 Hz, 1H), 5.00 (s, 2H), 4.55 (t, *J* = 4.8 Hz, 2H), 3.79 (t, *J* = 4.8 Hz, 2H). HRMS-ESI+: [M + H]+ calcd for $C_{21}H_{16}F_3N_3O_3$, 416.1216; found, 416.1213.

Automated Ion Channel Assays. The late sodium current (late I_{Na}) and peak sodium current (peak I_{Na}) assays were performed at room temperature on the QPatch automated electrophysiology platform (Sophion Bioscience, Copenhagen, Denmark), which used the whole cell patch clamp technique to measure currents through the cell membrane. Series resistance compensation was set to 100%, and series resistance and whole-cell compensation were performed automatically and currents were digitized at 25 kHz.

Cardiac hNa$_V$1.5 Assays. HEK293 cells stably expressing the human Na_v1.5voltage-gated sodium channel (Millipore, Billerica, MA)

DOI: 10.1021/acs.jmedchem.6b00939
J. Med. Chem. XXXX, XXX, XXX−XXX

were used to measure the block of I_{Na} at resting membrane potential of −120 mV. For the late I_{Na} assay, a voltage step from the resting membrane potential to −20 mV for 220 ms was performed at a stimulating frequency of 0.1 Hz. To improve assay signal-to-noise, late I_{Na} was enhanced using continuous application of tefluthrin (TEF, 10 μM) in the extracellular and intracellular solutions. Late I_{Na} was measured as the magnitude of I_{Na} during the end phase of the voltage step (210−220 ms). The extracellular solution was (in mM): 140 NaCl, 4 KCl, 1.8 $CaCl_2$, 0.75 $MgCl_2$, and 5 HEPES with pH adjusted to 7.4 using NaOH. The intracellular solution was (in mM): 120 CsF, 20 CsCl, 5 EGTA, 5 HEPES, and pH adjusted to 7.4 with CsOH. For the peak I_{Na} assay, a voltage step from the resting membrane potential to −20 mV for 20 ms was performed at a stimulating frequency of 0.1 Hz. This protocol was performed in control solution and after the superfusion of compound containing solution. The extracellular solution was (in mM): 40 NaCl, 100 choline Cl, 4 KCl, 1.8 $CaCl_2$, 0.75 $MgCl_2$ and 5 HEPES with pH adjusted to 7.4 using NaOH. The intracellular solution was (in mM): 120 CsF, 20 CsCl, 5 EGTA, 5 HEPES, and pH adjusted to 7.4 with CsOH.

hERG Assay. CHO−hERG DUO cells stably expressing the human ERG (*Ether-à-go-go* gene) K_V11.1 voltage-gated potassium channel were obtained from Sophion. Inhibition of peak tail current was measured from a holding potential of −80 mV. The voltage protocol consisted of two contiguous steps: first a step to +20 mV for 4.8 s followed by step to −40 mV for 5 s with a sweep frequency of 0.0667 Hz. Peak tail current IK was measured at the start of the step to −40 mV. This protocol was performed in control solution and after the superfusion of compound containing solution. Then 1 μM Cisapride solution was added near the end to define the baseline. The external recording solution was (in mM): 140 NaCl, 4 KCl, 1.8 $CaCl_2$, 1 $MaCl_2$, 10 HEPES, and 10 glucose. The internal recording solution was (in mM): 120 KCl, 31.25/10 KOH/EGTA, 10 HEPES, 5.374 $CaCl_2$, 1.75 $MgCl_2$, 4 Na_2-ATP.

Manual Ion Channel Assays for Non-Cardiac Na_V1.X Channels. Assays were performed at room temperature using a manual patch clamp in the whole-cell configuration using a MultiClamp 700B amplifier, Digidata 1400 digitizer, and pClamp 10 software (Molecular Devices, Sunnyvale, CA, USA). Series resistance was compensated 90% to ensure that the command potential was reached within microseconds with a voltage error <2 mV. Leak currents were subtracted by using an online P/4 procedure. Currents were low-pass Bessel filtered at 4 kHz and digitized at 50 kHz. The bath solution contained (mM): 140 NaCl, 4 KCl, 1.8 $CaCl_2$, 1 $MgCl_2$, 10 dextrose, and 10 HEPES, with a pH of 7.35. The pipet solution consisted of (mM) 10 NaF, 110 CsF, 20 CsCl, 2 EGTA, and 10 HEPES, with a pH of 7.35. Inhibition was assessed using a train of 50 square voltage steps (P_1 to P_{50}) from a holding potential of −120 mV to a test potential of 0 mV (20 ms) at a frequency of either 10 Hz. The ratio P50/P1 obtained in the presence of drug was normalized to the ratio obtained in the absence of drug (Control) to calculate the degree of inhibition.

Isolated Rabbit Heart Assay. Animal use was approved by the Institutional Animal Care and Use Committee of Gilead Sciences (Fremont, CA). New Zealand White female rabbits, weighing 2.5−3.5 kg, were sedated then anesthetized using IM and IV injections, respectively, of xylazine and ketamine. The heart was excised and placed in a modified Krebs−Heinsleit (K−H) solution (pH 7.4, gassed with 95% O_2 and 5% CO_2). The K−H solution contained (in mM): 118 NaCl, 2.8 KCl, 1.2 KH_2PO_4, 2.5 $CaCl_2$, 0.5 $MgSO_4$, 2.0 sodium pyruvate, 5.5 glucose, 0.57 Na_2EDTA, and 25 $NaHCO_3$. The aorta was cannulated and the heart was perfused by the method of Langendorff with K−H solution warmed to 36.5 °C. To ensure capture during pacing, the right atrial wall was partially removed and complete atrioventricular block was induced by thermoablation of the atrioventricular nodal area. A bipolar Teflon-coated electrode was placed on the right ventricular septum to pace the heart. Electrical stimuli, 2 ms in width and 3-fold threshold amplitude, were delivered to the pacing electrode at a frequency of 1 Hz using EP-4 stimulator (EP MedSystems, ST. JUDE MEDICAL). After initiation of ventricular pacing, a 30−50 min period was allowed for equilibration of heart rhythm. Pressure-contact Ag-AgCl MAP electrodes were placed on the epicardial ventricular free wall below the level of the atrial−ventricular valve at the base of the left ventricle. Electrical signals were amplified, filtered, and digitized in real time using a BIOPAC Systems MP 150 signal processor and displayed on a computer screen by AcqKnowledge 4.2 for MP150 software (BIOPAC Systems Inc.). The duration of the monophasic action potential at 90% repolarization ($MAPD_{90}$) was used to monitor left ventricular repolarization. $MAPD_{90}$ was first prolonged by the perfusion of the heart with ATX-II to activate late I_{Na}. The degree of $MAPD_{90}$ shortening back to baseline was measured at steady-state following compound perfusion.

Ischemia-Induced ECG S−T Segment Elevation by LAD Ligation in Rabbits. Female New Zealand rabbits (3.0−4.0 kg) were purchased from Western Oregon Rabbitry. Animals were housed on a 12 h light and dark cycle and received standard laboratory chow and water. All experiments were performed in accordance with the Guide for the Care and Use of Laboratory Animals published by The National Research Council and with the experimental protocol approved by the Institutional Animal Care Committee of Gilead Sciences, Inc.

Rabbits were anesthetized with ketamine (35 mg/kg) and xylazine (5 mg/kg) intramuscular injection (IM). A tracheotomy was performed, and the trachea was intubated with an endotracheal tube. The animal was ventilated with room air supplemented with oxygen using a pressure control animal ventilator (Kent Scientific Corp., Torrington, CT) at a respiratory rate of 40 strokes/min and peak inspiration pressure of 10 mmH_2O, which was adjusted to keep blood gases and pH within the physiological range (iSTAT clinic analyzer, Heska Corp.; Waukesha, WI). The left femoral artery was cannulated for the measurement of blood pressure (BP). Blood samples were also withdrawn from femoral artery. The right external jugular vein was cannulated for drug/vehicle administration. Needle electrodes were inserted subcutaneously into the limbs for recording of the surface electrocardiogram (ECG). The heart was exposed via an incision in the fourth intercostal space (fourth and/or fifth ribs were cut for a clear surgical vision). The chest was opened and a pericardial cradle was formed using four retractors. A coronary artery occluder, comprised of a snare made of 5 cm PE-10 tubing with a 6−0 Prolene polypropylene suture in it, was placed loosely around the left anterior descending artery (LAD) at its origin. Two unipolar electrodes, made with Teflon coated silver wire attached to a small patch of filter paper, were attached on the surface of the ischemic and normal regions of the left ventricle to record epicardial electrocardiogram. Reference electrodes were placed in the open incision of the neck. The body temperature of the animal was monitored via a rectal thermometer and maintained at 37−40 °C by adjusting the surface temperature of the surgical table. Regional ischemia (15 min) was induced by ligating the LAD, followed by 15 min of reperfusion caused by releasing the ligation. BP and ECG were monitored and recorded continuously using a computer data acquisition system (PowerLab, AD Instruments; Mountain View, CA). S−T segment height in both epicardial and surface ECG, and PR, QRS, and QT interval in surface ECG was analyzed using an ECG analysis module (AD Instruments, Mountain View, CA).

The heart was excised at the end of the experiment, and the LAD was religated. The ischemic area was visualized by perfusing the heart with 1% Evans blue in saline and calculated as a percentage of total ventricular weight. Rabbits with ischemic area less than 10% or larger than 25% were excluded from the analysis.

Experimental Protocol. Animals were randomly assigned to vehicle, GS-compound groups. After 30 min of dosing, the heart was subjected to 15 min of ischemia followed by 15 min of reperfusion.

Blood samples were collected at 1, 5, 10, 30, and 60 min after drug administration for determination of plasma concentrations of the compound. Plasma concentrations of GS compound were determined using a high performance liquid chromatograph−tandem mass spectrometric (LC/MS/MS).

The **20** dose-dependently prevented the ischemia-induced S−T elevation. The area under curve (AUC) for the S−T segment height

DOI: 10.1021/acs.jmedchem.6b00939
J. Med. Chem. XXXX, XXX, XXX−XXX

was reduced (vs control) by 38% and 88% at 0.28 and 0.52 μM plasma concentration of **20**. At the plasma concentration levels studied, **20** had no significant effect on blood pressure (BP), heart rate (HR), and ECG intervals prior to the ischemia.

Similarly, **4** dose-dependently prevented the ischemia-induced ST elevation. The area under curve (AUC) for the S−T segment height was reduced (vs control) by 55% and 93% at 0.25 and 0.5 μM, respectively, and plasma concentration of compound of **4**. At the plasma concentration levels studied, compound **4** had no significant effect on blood pressure (BP), heart rate (HR), and ECG intervals prior to the ischemia.

Ischemia-Induced Arrhythmia by LCX Ligation in Rabbits. Female New Zealand rabbits (3.0−4.0 kg) were purchased from Western Oregon Rabbit Company. Animals were housed on a 12 h light and dark cycle and received standard laboratory chow and water ad libitum. All experiments were performed in accordance with the Guide for the Care and Use of Laboratory Animals published by National Research Council and with the experimental protocol approved by the Institutional Animal Care Committee of Gilead Sciences, Inc. Rabbits were anesthetized with sodium pentobarbital given as an intravenous injection of 30 mg/kg followed by IV infusion at 15 mg/kg/h. A tracheotomy was performed, and the trachea was intubated with an endotracheal tube. The animal was ventilated with room air supplemented with oxygen using a pressure control animal ventilator (Kent Scientific Corp., Torrington, CT) at a respiratory rate of 40 strokes/min and peak inspiration pressure of 10 mmH_2O, which was adjusted to keep blood gases and pH within the physiological range (iSTAT clinic analyzer; Heska Corp., Waukesha, WI). The left femoral artery was cannulated for the measurement of blood pressure (BP). Blood samples were also withdrawn from femoral artery. The right external jugular vein was cannulated for drug/vehicle administration. Needle electrodes were inserted subcutaneously into the limbs for recording of the surface electrocardiogram (ECG). The heart was exposed via an incision at the fourth intercostal space (fourth and/or fifth ribs were cut for a clear surgical vision). The chest was opened, and a pericardial cradle was formed using four retractors. A coronary artery occluder, comprised of a snare made of 5 cm PE-10 tubing with a 6−0 prolene polypropylene suture in it, was placed loosely around the LCX 2−3 mm from its origin. The body temperature of the rabbit was monitored via a rectal thermometer and maintained between 37 and 40 °C by adjusting the surface temperature of the surgical table. Regional ischemia (30 min) was induced by ligating the LCX. BP and ECG were monitored and recorded continuously using a computerized data acquisition system (PowerLab; AD Instruments, Mountain View, CA). Incidences of ventricular tachycardia (VT) and ventricular fibrillation (VF) were examined during the ischemia period.

The heart was excised at the end of the experiment. The ischemic area was visualized by perfusing the heart with 1% Evans Blue in saline and calculated as a percentage of the total ventricular weight. Hearts with ischemic area less than 25% or larger than 50% were excluded from the analysis.

Experimental Protocol. Animals were randomly assigned to vehicle or GS compound groups. At 30 min after the dose of GS compounds, the heart was subjected to 30 min of ischemia. Blood samples were collected at 1, 5, 10, 30, and 60 min after drug administration for determination of plasma concentrations of the compound. Plasma concentrations of GS compound were determined using a high performance liquid chromatograph−tandem mass spectrometry (LC/MS/MS).

■ ASSOCIATED CONTENT

Supporting Information

The Supporting Information is available free of charge on the ACS Publications website at DOI: 10.1021/acs.jmedchem.6b00939.

Experimental for compounds **22**−**40**, additional pharmacological data for **4** including ion channel panel, in vitro selectivity panel results, methoxyamine−clofilium induced VT−VF model with **4**, mexilitine data in a LCX ligation model of VT−VF, details of homology model including sequence analysis of sodium channel isoforms (PDF)

Molecular formula strings (CSV)

■ AUTHOR INFORMATION

Corresponding Author

*Phone: 650-522-6360. E-mail: Jeff.Zablocki@Gilead.com.

Notes

The authors declare no competing financial interest.

■ ACKNOWLEDGMENTS

We thank John Shryock and Lin Wu for helpful discussions. All authors were fully supported by Gilead Sciences Inc. with no external funding of the research described.

■ ABBREVIATIONS USED

Å, angstrom; br s, broad singlet; CACO-2, heterogeneous human epithelial colorectal adenocarcinoma; CNS, central nervous system; Cyp, cytochrome P450; d, doublet; hERG, human *Ether-à-go-go*-related gene; HCM, hypertrophic cardiomyopathy; HEK-293, human embryonic kidney cell; (Hz), hertz; IHD, ischemic heart disease; IC_{50}, inhibitory concentration$_{50}$; IH assay, isolated heart assay; late I_{Na}, late sodium current; LAD, left anteriorior descending; LQT-3 syndrome, long QT-3 syndrome; $MAPD_{90}$, monophasic action potential duration$_{90}$; MARISA study, Monotherapy Assessment of Ranolazine in Stable Angina Study; ms, milliseconds; m, multiplet; NMR, nuclear magnetic resonance; peak I_{Na} current, peak cardiac sodium current; ppm, parts per million; q, quartet; ROS, reactive oxygen species; ATX-II, sea anemone toxin II; SAR, structure−activity relationship; rabbit ΔS−T, rabbit change in S−T segment elevation during ischemia; s, singlet; SA, sinoatrial; TdP, Torsades des Pointes; t, triplet; US, United States; VT−VF, ventricular tachycardia−ventricular fibrillation; V_{ss}, volume steady state

■ REFERENCES

(1) Fang, J.; Shaw, K. M.; Keenan, N. L. Prevalence of coronary heart disease-United States, 2006−2010. *MMWR Morb. Mortal. Wkly. Rep.* **2011**, *60*, 1377−1381.

(2) Kochanek, K. D.; Xu, J.; Murphy, S. L.; Minin, A. O.; Kung, H. C. Deaths: preliminary data for 2010. *National Vital Statistics Report* **2012**, *60*, 1−52.

(3) Banon, D.; Filion, K. B.; Budlovsky, T.; Franck, C.; Eisenberg, M. J. The usefulness of ranolazine for the treatment of refractory chronic stable angina pectoris as determined from a systematic review of randomized controlled trials. *Am. J. Cardiol.* **2014**, *113*, 1075−1082.

(4) Zaza, A.; Belardinelli, L.; Shryock, J. C. Pathophysiology and pharmacology of the cardiac "late sodium current. *Pharmacol. Ther.* **2008**, *119*, 326−339.

(5) Le Grand, B.; Vie, B.; Talmant, J.; Coraboeuf, E.; John, G. W. Alleviation of contractile dysfunction in ischemic hearts by slowly inactivating Na+ current blockers. *Am. J. Physiol.: Heart Circ. Physiol.* **1995**, *269*, H533−H540.

(6) Antzelevitch, C.; Belardinelli, L.; Zygmunt, A. C.; Burashnikov, A.; Di Diego, J. M.; Fish, J. M.; Cordeiro, J. M.; Thomas, G. Electrophysiological effects of ranolazine, a novel antianginal agent with antiarrhythmic properties. *Circulation* **2004**, *110*, 904−910.

(7) Chaitman, B. R.; Skettino, S. L.; Parker, J. O.; Hanley, P.; Meluzin, J.; Kuch, J.; Pepine, C. J.; Wang, W.; Nelson, J. J.; Hebert, D. A.; Wolff, A. A. Anti-ischemic effects and long-term survival during

DOI: 10.1021/acs.jmedchem.6b00939
J. Med. Chem. XXXX, XXX, XXX−XXX

ranolazine monotherapy in patients with chronic severe angina. *J. Am. Coll. Cardiol.* **2004**, *43*, 1375−1382.
(8) Fredj, S.; Sampson, K. J.; Liu, H.; Kass, R. S. Molecular basis of ranolazine block of LQT-3 mutant sodium channels: evidence for site of action. *Br. J. Pharmacol.* **2006**, *148*, 16−24.
(9) Catteral, W. A.; Goldin, A. L.; Waxman, S. G. International union of pharmacology. XLVII. nomenclature and structure-function relationships of voltage-gated sodium channels. *Pharmacol. Rev.* **2005**, *57*, 397−409.
(10) Abelman, M.; Elzein, E.; Jiang, R.; Kalla, R.; Kobayashi, T.; Li, X.; Perry, T. Fused heterocyclic compounds as ion channel modulators. WO2010056527, May 20, 2010.
(11) Koltun, D. O.; Parkhill, E. Q.; Elzein, E.; Kobayashi, T.; Notte, G.; Jiang, R. H.; Kalla, R.; Li, X.; Perry, T.; Avila, B.; Wang, W. Q.; Smith-Maxwell, C.; Dhalla, A. K.; Rajamani, S.; Shryock, J.; Mollova, N.; Stafford, B.; Tang, J.; Belardinelli, L.; Zablocki, J. A. Discovery of triazolopyridine GS-458967, a late sodium current inhibitor (Late INai) of the cardiac NaV 1.5 channel with improved efficacy and potency relative to ranolazine. *Bioorg. Med. Chem. Lett.* **2016**, *26*, 3202−3206.
(12) Kobayashi, T.; Koltun, D.; Notte, G.; Parkhill, E.; Zablocki, J. Fused heterocyclic compounds as ion channel modulators. WO 2012/003392, January 5, 2012.
(13) Koltun, D. O.; Parkhill, E. Q.; Elzein, E.; Kobayashi, T.; Jiang, R. H.; Li, X.; Perry, T. D.; Avila, B.; Wang, W. Q.; Hirakawa, R.; Smith-Maxwell, C.; Wu, L.; Dhalla, A. D.; Rajamani, S.; Mollova, N.; Stafford, B.; Tang, J.; Belardinelli, L.; Zablocki, J. A. Discovery of triazolopyridinone GS-462808, a late sodium current inhibitor (Late INai) of the cardiac $Na_v1.5$ channel with improved efficacy and potency relative to ranolazine. *Bioorg. Med. Chem. Lett.* **2016**, *26*, 3207−3211.
(14) Belardinelli, L.; Liu, G.; Smith-Maxwell, C.; Wang, W. Q.; El-Bizri, N.; Hirakawa, R.; Karpinski, S.; Li, C. H.; Hu, L.; Li, X. J.; Crumb, W.; Wu, L.; Koltun, D.; Zablocki, J.; Yao, L.; Dhalla, A. K.; Rajamani, S.; Shryock, J. C. A novel, potent, and selective inhibitor of cardiac late sodium current suppresses experimental arrhythmias. *J. Pharmacol. Exp. Ther.* **2013**, *344*, 23−32.
(15) Corkey, B. K.; Elzein, E.; Jiang, R. H.; Kalla, R. V.; Koltun, D.; Li, X.; Martinez, R.; Parkhill, E. Q.; Perry, T.; Zablocki, J.; Venkataramani, C.; Graupe, M.; Guerrero, J. Fused benzoxazepinones as ion channel modulators. WO 2013/006485, January 10, 2013.
(16) Corkey, B. K.; Elzein, E.; Jiang, R. H.; Kalla, R. V.; Koltun, D.; Li, X.; Martinez, R.; Parkhill, E. Q.; Perry, T.; Zablocki, J.; Venkataramani, C.; Graupe, M.; Guerrero, J. Fused heterocyclic compounds as sodium channel modulators. WO 2012/154760, November 15, 2012.
(17) Smart, B. E. Fluorine substituent effects (on bioactivity). *J. Fluorine Chem.* **2001**, *109*, 3−11.
(18) Muller, K.; Faeh, C.; Diederich, F. Fluorine in pharmaceuticals: looking beyond intuition. *Science* **2007**, *317*, 1881−1886.
(19) Muller, K. Simple vector considerations to assess the polarity of partially fluorinated alkyl and alkoxy groups. *Chimia* **2014**, *68*, 356−362.
(20) Payandeh, J.; Scheuer, T.; Zheng, N.; Catterall, W. A. The crystal structure of a voltage-gated sodium channel. *Nature* **2011**, *475*, 353−358.
(21) Jensen, M.Ø.; Jogini, V.; Borhani, D. W.; Leffler, A. E.; Dror, R. O.; Shaw, D. E. Mechanism of voltage gating in potassium channels. *Science* **2012**, *336*, 229−233.
(22) Rohl, C. A.; Boeckman, F. A.; Baker, C.; Scheuer, T.; Catterall, W. A.; Klevit, R. E. Solution structure of the sodium channel inactivation gate. *Biochemistry* **1999**, *38*, 855−861.
(23) Heinemann, S. H.; Terlau, H.; Stühmer, W.; Imoto, K.; Numa, S. Calcium channel characteristics conferred on the sodium channel by single mutations. *Nature* **1992**, *356*, 441−443.
(24) Moss, A. J.; Zareba, W.; Schwarz, K. Q.; Rosero, S.; McNitt, S.; Robinson, J. L. Ranolazine shortens repolarization in patients with sustained inward sodium current due to type-3 Long-QT syndrome. *J. Cardiovasc. Electrophysiol.* **2008**, *19*, 1289−1293.
(25) Zareba, W.; Rosero, S.; Zeng, D.; Moss, A. J.; Couderc, J.-P.; Layug, B.; Belardinelli, L. Sustained QTc shortening by GS-6615 in patients with LQT3. *Heart Rhythm Society 35th Annual Meeting May 7−10, 2014, San Francisco*, 2014; Abstract AB-34-05.
(26) Le Grand, B.; Pignier, C.; Létienne, R.; Cuisiat, F.; Rolland, F.; Mas, A.; Vacher, B. Sodium late current blockers in ischemia reperfusion: is the bullet magic? *J. Med. Chem.* **2008**, *51*, 3856−3866.
(27) Le Grand, B.; Pignier, C.; Létienne, R.; Colpaert, F.; Cuisiat, F.; Rolland, F.; Mas, A.; Borras, M.; Vacher, B. Na+ currents in cardioprotection: better to be late. *J. Med. Chem.* **2009**, *52*, 4149−4160.
(28) Echt, D. S.; Liebson, P. R.; Mitchell, L. B.; Peters, R. W.; Obias-Manno, D.; Barker, A. H.; Arensberg, D.; Baker, A.; Friedman, R.; Greene, H. L.; Huther, M. L.; Richardson, D. W Mortality and morbidity in patients receiving encainide, flecainide, or placebo — the Cardiac Arrhythmia Suppression Trial. *N. Engl. J. Med.* **1991**, *324*, 781−788.
(29) Diamond, I.; Belardinelli, L.; Shryock, J.; Rajamani, S. Use of ranolazine for treating pain. WO 2009/100380 Aug 13, 2009.

DOI: 10.1021/acs.jmedchem.6b00939
J. Med. Chem. XXXX, XXX, XXX−XXX